applied sciences

MDPI

Article

Tannic Acid-Loaded Hydroxyapatite Carriers for Corrosion Protection of Polyolefin-Coated Carbon Steel

Roma Raj [1,*], Ramazan Kahraman [2], Abdul Shakoor [3], Fatima Montemor [1] and Maryna Taryba [1]

[1] Centro de Química Estrutural, Instituto Superior Técnico, Universidade de Lisboa, 1049-001 Lisboa, Portugal
[2] Department of Chemical Engineering, Qatar University, Doha 2713, Qatar
[3] Center for Advanced Materials, Qatar University, Doha 2713, Qatar
* Correspondence: roma.raj@tecnico.ulisboa.pt

Abstract: In this study, pH-sensitive hydroxyapatite particles loaded with tannic acid were incorporated in polyolefin-based coatings for the corrosion protection of carbon steel. Transmission electron microscopy (TEM), X-ray diffraction (XRD), Fourier transform infrared spectroscopy (FTIR), and thermogravimetric analysis (TGA) were used to characterize the hydroxyapatite particles loaded with tannic acid (Tannic-HAP). Electrochemical impedance spectroscopy (EIS) was employed to study the protective performance of the reference and modified polyolefin coatings. The results suggest that modified coatings showed improved corrosion performance compared to the unmodified coatings. The combination of tannic acid and hydroxyapatite contributed to a more effective protection of coated carbon steel.

Keywords: tannic acid; protective coating; polyolefin; hydroxyapatite; carbon steel; corrosion

Citation: Raj, R.; Kahraman, R.; Shakoor, A.; Montemor, F.; Taryba, M. Tannic Acid-Loaded Hydroxyapatite Carriers for Corrosion Protection of Polyolefin-Coated Carbon Steel. *Appl. Sci.* **2022**, *12*, 10263. https://doi.org/10.3390/app122010263

Academic Editor: Ioannis Kartsonakis

Received: 25 April 2022
Accepted: 5 October 2022
Published: 12 October 2022

1. Introduction

One of the most effective ways to control corrosion is by the application of organic coatings. Anti-corrosion coatings are typically thick, applied on several layers, and impermeable against aggressive species, providing an effective physical barrier between the bare metal and the external environment. Nevertheless, coatings always contain pores, pinholes, and other defects that create preferential paths for the uptake of moisture, oxygen, and aggressive species. Over time, these species may reach the bare metal and corrosion starts, inducing local coating degradation and further corrosion propagation. This problem can be more serious when the coated steel is damaged.

To mitigate corrosion propagation, coatings must be modified with anti-corrosion pigments. These pigments must ensure that corrosion is efficiently inhibited especially when the coating is damaged. Over many years, different chromate-containing pigments were well-established corrosion inhibitors but in the early 21st century, many regulations started to restrict their use due to their high toxicity and carcinogenic effects [1–3]. As a consequence, important research efforts have been made in the search for novel and more environmentally friendly corrosion inhibitors. Over the past two decades, several alternative inorganic inhibitors [4–6] have been investigated such as molybdates [7], vanadates [8], permanganates [9], and different rare earth metals such as lanthanum [10] and cerium [11]. In addition, several organic [12–14] inhibitors were examined such as 8-hydroxyquinoline [15], benzotriazole [16], amines [17], carboxylic acids [18], mercaptobenzothiazole [19], salicyladoxime [20], and quinaldic acid [21]. However, some of these inhibitors are also under straight vigilance and some are already considered non-recommended ones. This means that the search for effective, environmentally friendly, and non-toxic corrosion inhibitors is still an actual and dynamic research field, particularly relevant to enable new generations of highly effective anti-corrosion coatings.

An easy way to formulate an anti-corrosion coating consists of the direct addition of the corrosion inhibitors directly into the coating formulation. Although this procedure

is well established for many conventional inorganic anti-corrosion pigments, unwanted side effects may arise when new inhibitors, particularly organic ones, are introduced in the coating formulations. These unwanted interactions may induce changes in the polymer matrix, weakening its barrier properties. Moreover, it is of paramount importance to avoid changes in the chemical nature of the inhibitor (e.g., due to side reactions with species present in the coating formulation) and to control early inhibitor de-activation or leaching from the coating. To minimize these effects, one possible route is the storage of the corrosion inhibitors in inorganic carriers with good compatibility with the coating formulation. These carriers are expected to sense certain stimuli in the coating or steel coating interface and use them to control the inhibitor delivery [22].

Molecules serving as organic inhibitors usually contain groups with nitrogen, oxygen, or sulfur, and therefore π electrons that play a key role in the adsorption of the inhibitors onto the metal surface where they can form protective layers that restrict the flow of aggressive species. The effectiveness of corrosion inhibition depends on several factors such as the condition of the metal surface, nature of the aggressive electrolyte, inhibitor concentration, and chemical nature of the inhibitor [13,23].

In the present work, a new anticorrosive system for carbon steel is proposed. The protective system consists of a polyolefin-based coating loaded with pH-sensitive hydroxyapatite (HAP) particles serving as carriers for tannic acid. The use of pH-sensitive HAP particles has a twofold role: on the one hand they dissolve slowly at a slightly acidic pH, releasing the tannic acid from the loaded carrier, and, on the other hand, they provide a source of soluble phosphate anions that contribute to forming protective phosphate-rich iron compounds. The dissolution is enabled by the local pH acidification that occurs at anodic sites due to hydrolysis of the iron cations [24]. Another important advantage is the low price of HAP particles that are also simple to prepare, non-toxic, and easily loaded with different organic corrosion inhibitors as reported elsewhere [25].

Tannic acid is a well-known corrosion inhibitor that can be derived from bio-renewable resources. This inhibitor has demonstrated interesting anti-corrosion properties when used as an additive in different coatings such as polyurethane [26,27]. Thus, in this work, the novel approach consists of the modification of HAP with tannic acid (an eco-friendly corrosion inhibitor) and its incorporation into a polyolefin formulation to enhance the corrosion protection performance.

The anti-corrosive performance of coated steel samples with and without artificial defects was studied in NaCl electrolytes using electrochemical impedance spectroscopy (EIS). The results demonstrate that the presence of HAP particles loaded with tannic acid in the coating delays the propagation of corrosion and, in the longer term, can provide effective corrosion protection.

2. Experiment

2.1. Materials and Chemicals

The following reagents were purchased from Sigma Aldrich: calcium nitrate tetrahydrate (99% purity), ammonium hydrogen phosphate (98% purity), tannic acid, ethylenediaminetetraacetic acid, and its disodium salt dihydrate. Sodium chloride was purchased from Carl Roth whereas absolute ethanol was ordered from AppliChem Panreac. All solutions were prepared using Deionized Millipore™ grade water. Commercial carbon steel plates (DC01 steel) were used.

2.2. Preparation of Tannic Acid-Loaded HAP Particles

2.2.1. Synthesis of Hydroxyapatite

Hydroxyapatite particles were synthesized according to a previously reported procedure [28]. In the first step, 0.2 g of EDTA and 0.2 M calcium nitrate were mixed and sonicated for 10 min. Then, 0.11 M ammonium hydrogen phosphate was poured slowly into the above-prepared solution using the IKA® Ultra Turrax® T18 at room temperature. The resulting solution was kept in a water bath for 4 h, at 60 °C. The pH of the solution

was adjusted to 12 using NaOH to enable precipitation. The precipitate was collected after 4 h and washed thoroughly with DI water and ethanol. The obtained particles were dried in the oven for 24 h at 50 °C and stored in a dry environment.

2.2.2. Loading of HAP Particles with Tannic Acid

Tannic acid was added to the 0.11 M ammonium hydrogen phosphate which also allows for better control of the morphology of HAP particles. After this step, the synthesis followed the same route as mentioned in Section 2.2.1.

2.3. Preparation of Polyolefin-Coated Carbon Steel Samples

Carbon steel samples were cut in 4 × 5 cm^2 standard size plates from the 0.7 mm thick commercial DC01 steel sheets. In a prior coating procedure, steel samples were degreased in acetone for 10 min under sonication and dried.

A polyolefin-based formulation, based on a commercial product (the detailed coating formulation cannot be disclosed due to commercial property) and adopted for research purposes was used to coat the steel samples. Two sets of coating were prepared. The first set was a blank (reference) coating, without any anti-corrosion pigments. The second one was the modified coating that contained 5 wt.% of tannic acid-loaded HAP particles. The modified coating solution was left overnight, and the steel samples were coated the next day using the dip-coating method. The curing of all coated samples was performed at 150 °C in an oven for 20 min.

3. Physicochemical Study of Particles and Coated Samples

3.1. Transmission Electron Microscopy

The blank and tannic acid-loaded HAP particles were characterized using a Hitachi H8100 transmission electron microscope at 200 kV.

3.2. X-ray Diffraction

Phase identification of the HAP particles before and after loading with tannic acid was performed by X-ray diffraction using a Bruker AXS-D8 Advance powder Diffractometer and the Cu-K_α radiation source (λ = 0.150619 nm).

3.3. Fourier Transform Infrared Spectroscopy (FTIR)

FTIR measurements were performed both on the blank and tannic acid-loaded HAP particles to further detail the chemical composition. A spectrometer equipped with Pike Technologies Miracle® ATR accessory at 8 cm^{-1} resolution was used for the experiments.

3.4. Thermogravimetric Analysis (TGA)

TG/DTG profiles were obtained to determine the amount of tannic acid-loaded in the HAP particles. A HITACHI STA7200 apparatus, at a heating rate of 10 °C·min^{-1} from 25 °C to 1000 °C, was used in a nitrogen atmosphere to carry out the experiments. Total organic carbon content, used for calculation of the tannic acid release at different pH values, was obtained employing the TOC analyzer Formacs™.

3.5. Electrochemical Studies

Electrochemical Impedance Spectroscopy

Electrochemical impedance spectroscopy (EIS) measurements were carried out using a Gamry 600+ Potentiostat in a Faraday cage to avoid electromagnetic interference. The experiments were performed in triplicate, in the frequency range of 50 kHz to 5 mHz in 0.05 M NaCl. The spectra were obtained under open circuit potential using a sinusoidal perturbation of 10 mV (rms) in a 3-electrodes electrochemical cell. It consisted of a Pt spiral serving as counter electrode-, a saturated calomel electrode (SCE) as reference electrode-, and the working electrode (coated steel samples). Studies were carried out on intact coatings and previously damaged coatings. The damage was a round defect of approximately

200 µm, created with a sharp knife. The size of the defect was controlled by optical microscopy. The aim was to achieve a well-controlled fast-track for corrosion propagation and its inhibition.

4. Results and Discussion

4.1. Characterization of the Hydroxyapatite Particles

Figure 1a,b show the TEM images of hydroxyapatite particles without and with tannic acid, respectively. The blank hydroxyapatite particles consist of packed nanorods with sizes varying from 50–150 nm that tend to form clusters with sizes up to several micrometers. Tannic acid-loaded HAP particles (Figure 1b) are thinner and longer compared to the blank HAP particles (Figure 1a). In fact, due to the shape and size of the thin rods, a larger quantity of corrosion inhibitors can be filled inside the rod-like particles. When the particles are loaded with tannic acid, this one seems to uniformly cover the particles. The amount of tannic acid loading will be discussed below in light of the TGA analysis.

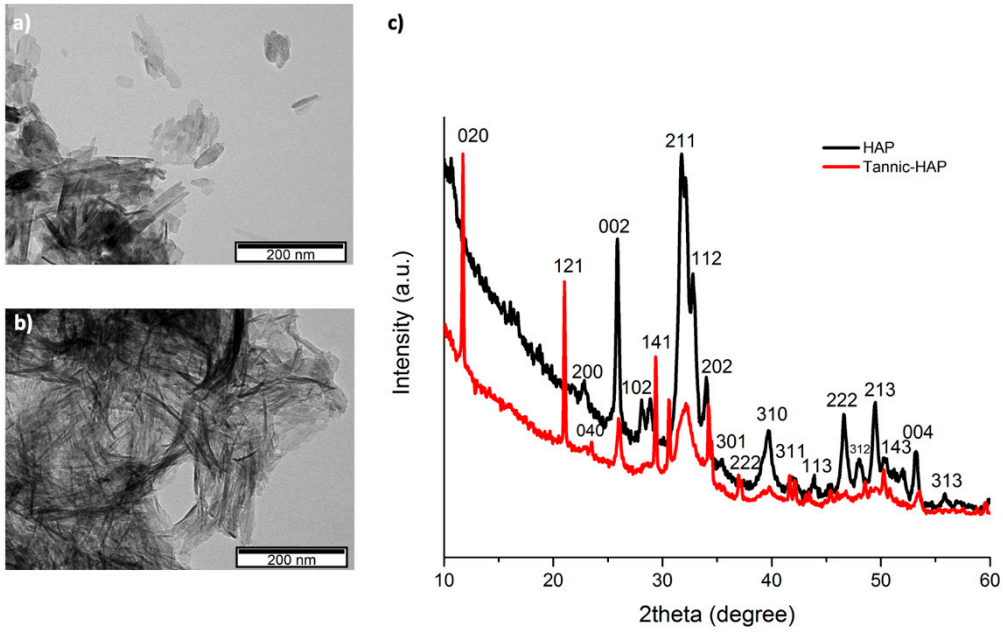

Figure 1. TEM images of (**a**) blank HAP particles, (**b**) HAP particles loaded with tannic acid, and (**c**) XRD analysis for blank and tannic acid-loaded HAP.

XRD was performed to study the structural properties of bare HAP particles and tannic acid-loaded HAP particles. The XRD results (Figure 1c) revealed the main crystalline peaks of blank hydroxyapatite particles which were in good agreement with pure hydroxyapatite particles according to the JCPDS card number 09-0432. The aligned peaks were (002), (102), (210), (211), (112), (202), (310), (213), and (004), and the main peaks were (002), (211), and (112) which can be assigned to the characteristic peaks for the HAP particles [29]. The same peaks were present in tannic acid-loaded HAP particles. Since tannic acid is non-crystalline, it can be assumed that the introduction of tannic acid in HAP particles is responsible for the changes in crystal planes and therefore, broader peaks were observed in the case of tannic acid-loaded HAP.

The presence of tannic acid was confirmed by ATR-FTIR (Figure 2a). Well-defined P-O stretching bands were located at 1056 cm^{-1}, 1085 cm^{-1}, and 1096 cm^{-1}. O-P-O bending bands were also found near 660 cm^{-1} and 520 cm^{-1} [30]. Near 3570 cm^{-1} and 632 cm^{-1}, it is possible to identify the stretching and bending bands of O-H [31].

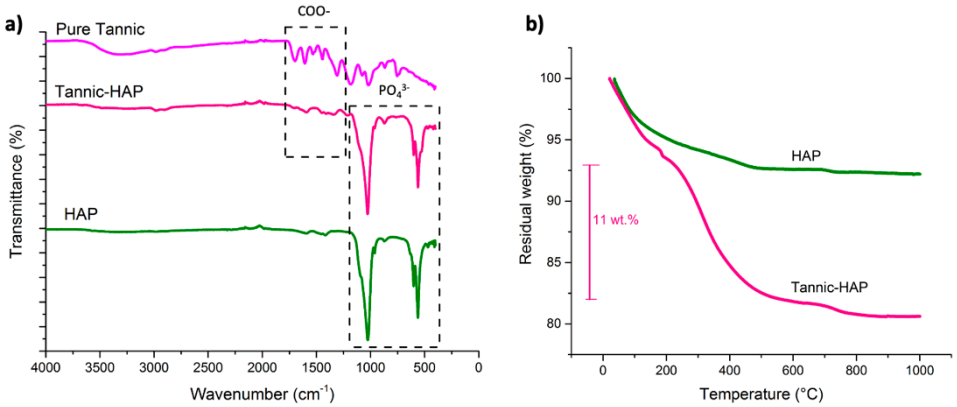

Figure 2. (**a**) FTIR for tannic acid, blank HAP, and tannic acid-loaded HAP; (**b**) TGA for blank HAP, tannic acid, and tannic acid-loaded HAP.

In the case of tannic acid-loaded HAP particles, O-H bands were observed near 3325 cm^{-1}. The bands near 2710 cm^{-1} and 1698 cm^{-1} correspond to the asymmetric stretch of C-H and C=O stretch, respectively. Aromatic C-O symmetrical stretch bands were detected near 1606 cm^{-1}. The bands spotted in the range 1443–1532 cm^{-1} can be assigned to aromatic C=C. The asymmetrical stretch of aromatic C-O is located at 1307 and 1177 cm^{-1}. C-O-C stretch bands were found near 1016 cm^{-1}. The band near 754 cm^{-1} corresponds to C-H. The fingerprints of tannic acid agreed with the expected bands for the pure tannic acid [32].

TG measurements were carried out to quantify the amount of tannic acid in the HAP particles and to study the thermal stability of the particles (Figure 2b). HAP particles showed thermal stability until 1000 °C. In the first step, mass losses assigned to loss of water, CO, CO_2, and breakdown of high molecular weight phenols into small chain fragments were expected. HAP particles may enter phase transformation into various phosphate groups after 600 °C, as previously discussed [28]. Tannic acid decomposition starts at 150 °C and it is expected to decompose until 600 °C [33]. Tannic acid-loaded HAP particles are evidenced in three regions: the first one at a lower temperature is due to water loss; the second region corresponds to the degradation of tannic acid; and the third one is due to the decomposition of HAP particles at higher temperatures. The TGA results allowed to estimate the tannic acid content in the HAP particles that was approximately 11%. This reveals a very interesting corrosion inhibition loading.

Release from the Particles

The dissolution of the hydroxyapatite particles is a complex process. These particles are expected to dissolve below pH 4, releasing the corrosion inhibitor; however, the process shows some reversibility. As the pH decreasing reversibility is more difficult and in the pH range below 3.5, no solid products are expected, as demonstrated in a previous work [25]. Figure 3 shows that the release of tannic acid occurred in all pH ranges, including in the weak alkaline region. A significant increase in the inhibitor release was observed when the pH decreased below 3 and a complete release (and dissolution) of the particles was observed. Although hydroxyapatite particles are not supposed to dissolve above pH 8, the release of tannic acid was also observed. This effect may be due to the release of the superficial inhibitor adsorbed on the surface or in the pores of the hydroxyapatite particles. This release of inhibitor may introduce some early leaching decreasing the availability of the inhibitor at the later stages of corrosion.

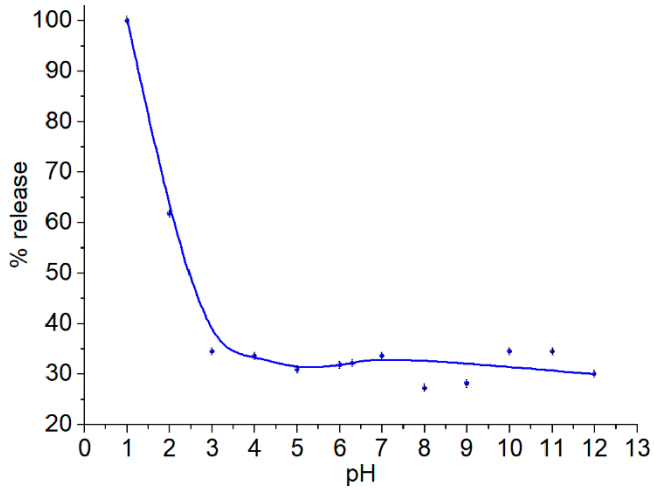

Figure 3. The release of inhibitors at different pH. Standard deviation was less than 0.9% for each depicted data point.

4.2. Corrosion Performance of Polyolefin Coated Steel Modified with Tannic Acid-HAP Particles

Electrochemical Impedance Measurements

EIS was used to investigate the barrier properties of reference coatings and coatings modified with HAP particles loaded with tannic acid. Changes in the high-frequency range can be correlated to the coating porosity and presence of defects or small pinholes. The coated steel samples were immersed for 30 days in 0.05 M NaCl. The thickness of the produced modified coatings and reference coatings was 18 ± 0.5 µm and 20 ± 0.5 µm, respectively.

Figure 4 shows sets of representative EIS Bode plots, obtained on the reference (blank polyolefin coating without additives) and modified coatings after immersion in 0.05 M NaCl for 30 days.

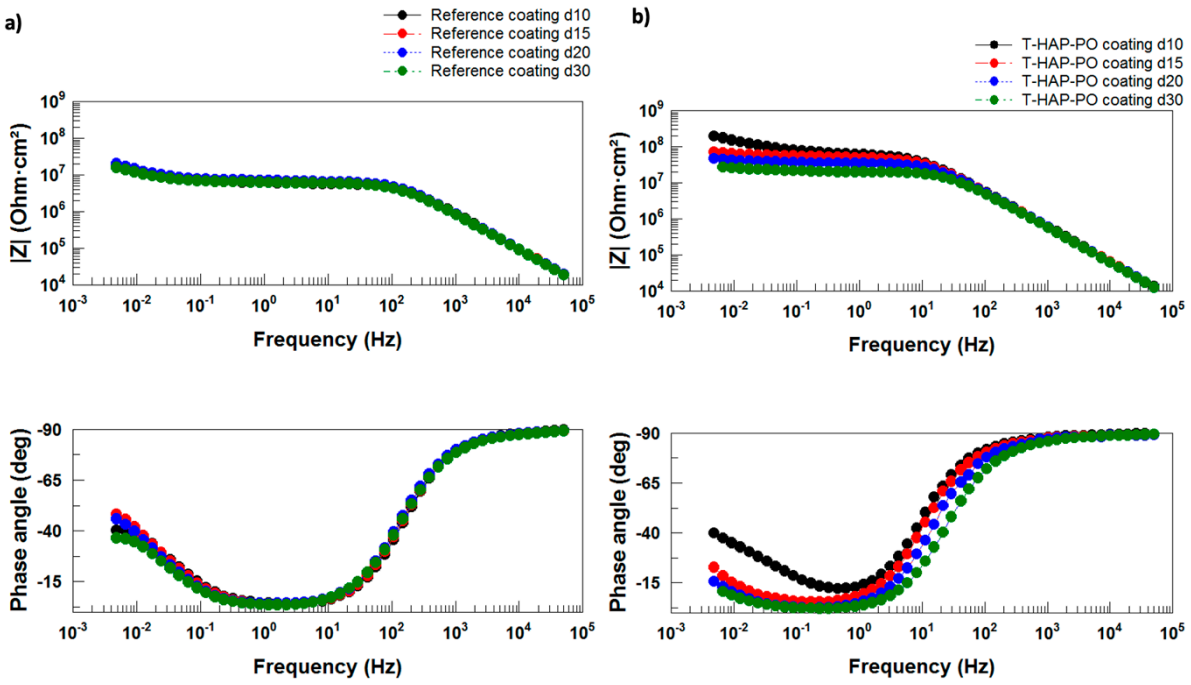

Figure 4. EIS Bode plots for the (**a**) reference coating and (**b**) coating modified with HAP particles loaded with tannic acid during immersion in 0.05 M NaCl.

Both coatings showed a very stable high-frequency capacitive loop from the early stage of immersion. The phase angle was more negative than −80° and approached −90° above 100 Hz for the modified coating. The same trend was observed for the blank coating but only above 1 kHz. The wider frequency range displaying phase angles close to −90° confirms the better barrier properties of the modified coating and accounts for a lower porosity compared to the blank coating. The overall impedance of the blank coating showed very stable values, around 10^7 Ohm·cm^2, since the start of the immersion test until its end.

The modified coatings behaved differently. The initial impedance values were above 10^8 Ohm·cm^2 and decayed slowly, remaining above 10^7 Ohm·cm^2 at the end of 30 days of immersion. Overall, this coating also showed very stable barrier properties, and the EIS results evidenced that the presence of HAP particles loaded with tannic acid did not have any detrimental effects.

To better detail the corrosion inhibition efficacy of the HAP loaded with tannic acid, a round-shaped defect, with a diameter of around 200 µm and reaching the bare metal, was created in the coated steel samples. The samples were studied for 5 days in 0.05 M NaCl. As expected, both coatings revealed a strong drop in the impedance values compared to the intact coatings—Figure 5. The high-frequency barrier was disrupted, and at medium frequencies, the time constant present in all the spectra can be assigned to the faradaic processes that occur at the steel interface. In both cases, at low frequencies, an incipient time constant points out the presence of mass transfer-controlled corrosion activity. The impedance values for both coatings were slightly different. The blank coating revealed impedance values around 10^5 Ohm·cm^2 that slowly decayed to half of this value after 5 days of immersion, while the modified coating showed impedance values initially around 10^6 Ohm·cm^2 that evidenced some fluctuations and a small drop after 5 days of immersion. Overall, the modified coating revealed impedance values that were approximately one order of magnitude above the blank coating, stating its superior corrosion protection performance. This was confirmed by the fitting results presented below in Figure 6c. These results demonstrate that even in the presence of a defect in the coating, the addition of HAP modified with tannic acid can slow down the corrosion activity and, consequently, the extent of the damage.

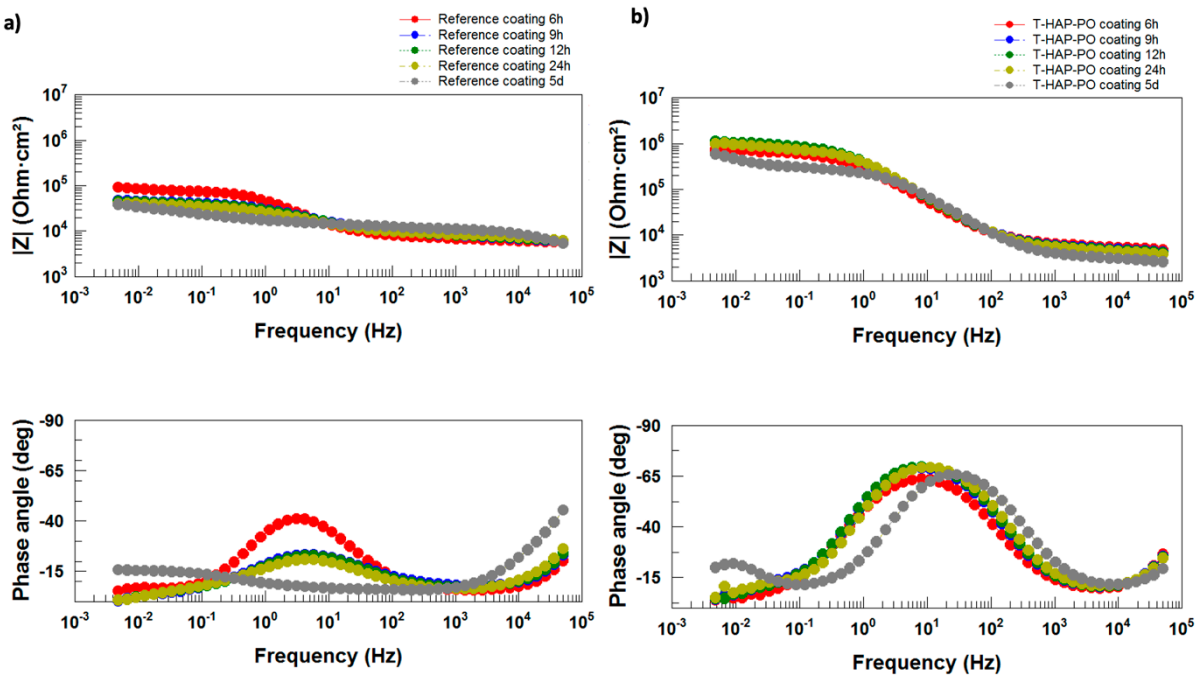

Figure 5. EIS Bode plots for the (**a**) reference coating and (**b**) coating modified with HAP particles loaded with tannic acid during immersion in 0.05 M NaCl with an artificial defect.

To better quantify the differences between the two non-damaged coatings, the spectra were simulated using the equivalent circuit presented in Figure 7. This equivalent circuit reflects two-time constants. The high-frequency time constant was introduced to account for the high-frequency barrier properties, while the CPEdl and Rct were used to simulate the low-frequency response, i.e., the interfacial activity at the steel coating interface. Constant phase elements (CPE) were used instead of capacitors. The fitting results are depicted in Figure 6.

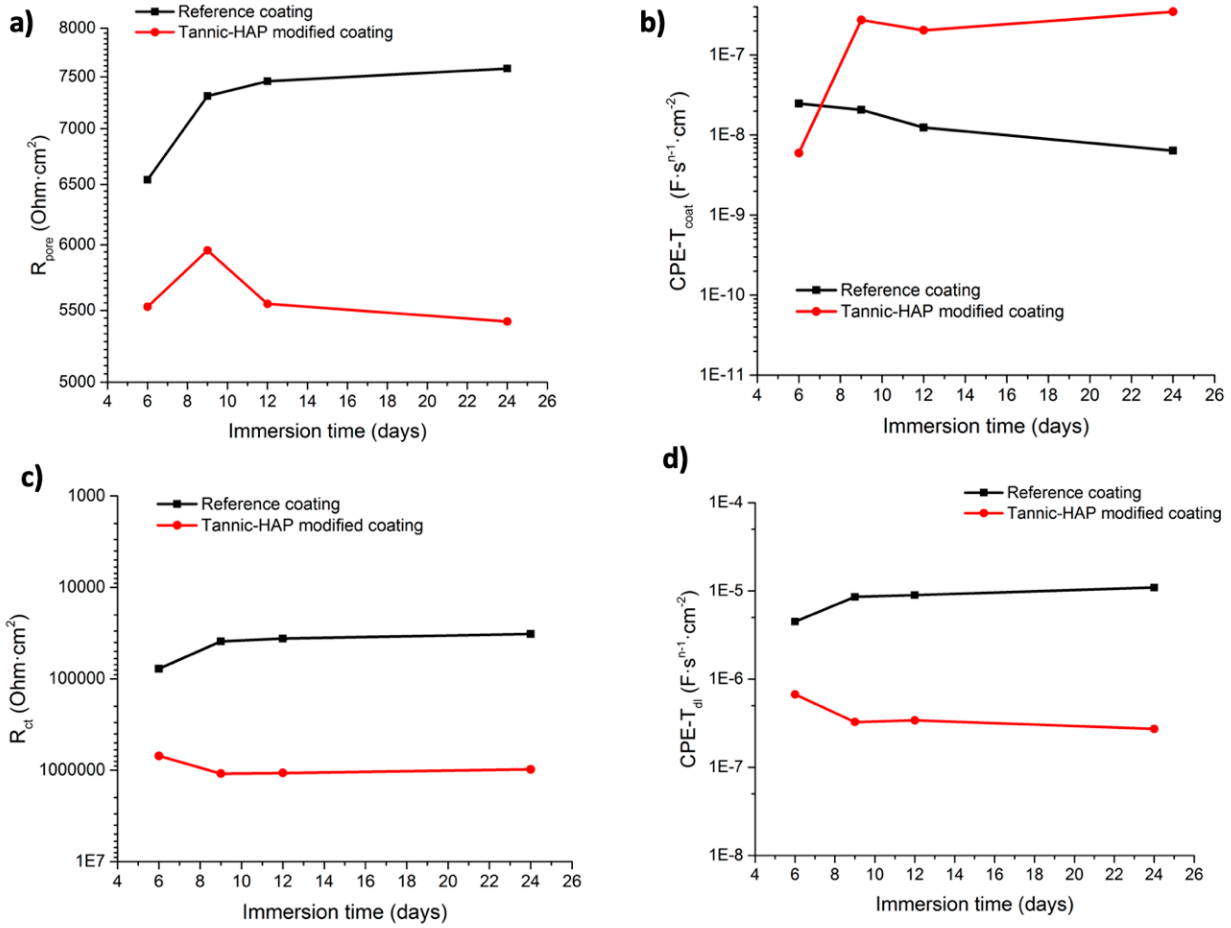

Figure 6. Evolution of the fitting parameters extracted from the numerical simulation of the experimental EIS data: (**a**) pore resistance; (**b**) admittance of the CPE for the coating; (**c**) charge transfer resistance; (**d**) admittance of the low-frequency CPE.

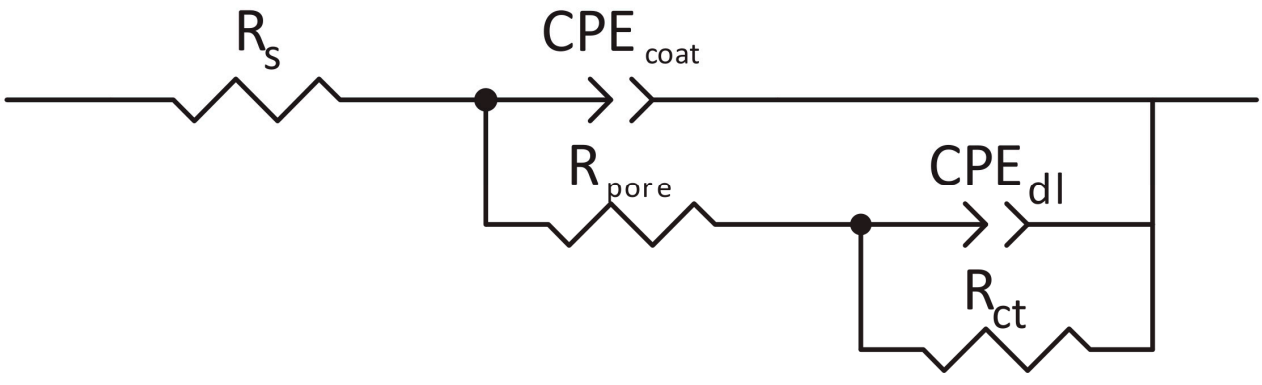

Figure 7. The equivalent circuit used to fit the experimental EIS data.

Figure 6a,b evidenced higher values of pore resistance and lower admittance values for the blank coating compared to the modified coatings.

The faradaic resistance values determined by fitting evidenced significant differences. In the modified coating (Figure 6c), the faradaic resistance increased after the first day of immersion attaining values around 1 MOhm.cm^2 and being very stable over the 5 days of testing. Concomitantly, the admittance of the CPE (Figure 6d) also remained stable and more than one order of magnitude below that of the blank coatings (Figure 6b).

Contrarily, the faradaic resistance in the blank coating showed a monotonous drop, decaying from 100 kOhm.cm^2 to 5 kOhm.cm^2 (Figure 6c). The trends observed in Figure 5 demonstrated that the modified coatings provide very effective barrier properties, with a higher and stable pore resistance as well as marked corrosion inhibition. It is observed that the faradaic resistance is more than one order of magnitude higher in the modified coating, evidencing that the corrosion process is effectively inhibited.

The positive effects related to modification of the coating with HAP loaded with tannic acid can be summarized as follows: the particles are compatible with polyolefin coatings and do not disrupt the original barrier properties. When the electrolyte and chloride ions reach the bare steel corrosion starts, local pH changes occur. Thus, the pH increases at the cathodic sites, while at the anodic sites the pH acidifies as a consequence of iron cations hydrolysis. HAP is sensitive to pH and may enter a slow dissolution process, as previously reported elsewhere [25]. During this process, the inhibitor can be released from the particles leading to the formation of protective species over the exposed steel. Additionally, phosphate ions released from HAP dissolution may form stable and protective compounds with iron hydroxides blocking anodic activity. These processes contribute to decreasing the corrosion activity in intact coatings, as observed in Figure 5. In fact, in non-damaged coatings, corrosion is likely to start at the bottom of the natural pores and the subsequent accumulation of protective species, including iron phosphate compounds, can block those small pores, significantly delaying corrosion propagation. However, when the coating is artificially damaged, corrosion is expected to start immediately after immersion, and due to iron cation hydrolysis, important acidification is likely to occur at the early stages. Under these conditions, the particles start to dissolve, releasing tannic acid that forms complexes onto the exposed surface, thus delaying corrosion activity. Concurrently, the formation of iron phosphate compounds will promote the formation of protective products.

5. Conclusions

This study demonstrates that hydroxyapatite particles can be loaded with a relatively high amount of tannic acid, an eco-friendly corrosion inhibitor. This system carries potential to be used as an anti-corrosion pigment in polyolefin coatings. The presence of the loaded particles does not damage the barrier properties of the coating that remain very stable as confirmed by electrochemical impedance spectroscopy. The anti-corrosion properties of the modified coating are evidenced by the increased and stable low-frequency impedance values that were more than one order of magnitude above those of the blank coating. Results obtained for artificially damaged coated samples reveal that the hydroxyapatite particles loaded with tannic acid can delay corrosion propagation at the early stages.

Author Contributions: Conceptualization, R.R.; Methodology, R.R.; Supervision, F.M.; Validation, F.M. and M.T.; Visualization, R.K. and A.S.; Writing—original draft, R.R.; Writing—review & editing, F.M. and M.T. All authors have read and agreed to the published version of the manuscript.

Funding: This research received no external funding.

Institutional Review Board Statement: Not applicable.

Informed Consent Statement: Not applicable.

Data Availability Statement: Not applicable.

Acknowledgments: This publication was made possible by NPRP13S-0120-200116 from the Qatar National Research Fund (a member of the Qatar Foundation). The authors from Centro de Química Estrutural acknowledge the financial support of Fundação para a Ciência e Tecnologia (UIDB/00100/2021, LA/P/0056/2020, and UIDP/00100/2021). Statements made herein are solely the responsibility of the authors. The authors acknowledge Dow Chemical Company (Bernhard Kainz, Global Application Development Leader Metal Packaging Coatings, Dow Coating Materials) for providing polyolefin CANVERA 1110 coating formulation; Voestalpine AG for providing carbon steel; Marta Alves (Instituto Superior Técnico) for conducting the XRD tests; Mário Vale (Instituto Superior Técnico) for performing TG/DTG studies.

Conflicts of Interest: The authors declare no conflict of interest.

References

1. Montemor, M.F. Functional and smart coatings for corrosion protection: A review of recent advances. *Surf. Coat. Technol.* **2014**, *258*, 17–37. [CrossRef]
2. Prabakaran, M.; Durainatarajan, P.; Ramesh, S.; Periasamy, V. Enhanced corrosion inhibition behavior of carbon steel in aqueous solution by Phosphoserine-Zn2+ system. *J. Adhes. Sci. Technol.* **2016**, *30*, 1487–1509. [CrossRef]
3. Sørensen, P.A.; Kiil, S.; Dam-Johansen, K.; Weinell, C.E. Anticorrosive coatings: A review. *J. Coat. Technol. Res.* **2009**, *6*, 135–176. [CrossRef]
4. Samiento-Bustos, E.; Rodriguez, J.G.G.; Uruchurtu, J.; Dominguez-Patiño, G.; Salinas-Bravo, V.M. Effect of inorganic inhibitors on the corrosion behavior of 1018 carbon steel in the LiBr + ethylene glycol + H2O mixture. *Corros. Sci.* **2008**, *50*, 2296–2303. [CrossRef]
5. Abd El Aal, E.E.; Abd El Wanees, S.; Farouk, A.; Abd El Haleem, S.M. Factors affecting the corrosion behaviour of aluminium in acid solutions. II. Inorganic additives as corrosion inhibitors for Al in HCl solutions. *Corros. Sci.* **2013**, *68*, 14–24. [CrossRef]
6. Moutarlier, V.; Neveu, B.; Gigandet, M.P. Evolution of corrosion protection for sol–gel coatings doped with inorganic inhibitors. *Surf. Coat. Technol.* **2008**, *202*, 2052–2058. [CrossRef]
7. Mu, G.; Li, X.; Qu, Q.; Zhou, J. Molybdate and tungstate as corrosion inhibitors for cold rolling steel in hydrochloric acid solution. *Corros. Sci.* **2006**, *48*, 445–459. [CrossRef]
8. Iannuzzi, M.; Young, T.; Frankel, G.S. Aluminum Alloy Corrosion Inhibition by Vanadates. *J. Electrochem. Soc.* **2006**, *153*, B533. [CrossRef]
9. Madden, S.B.; Scully, J.R. Inhibition of AA2024-T351 Corrosion Using Permanganate. *J. Electrochem. Soc.* **2014**, *161*, C162. [CrossRef]
10. Seddik, N.B.; Raissouni, I.; Draoui, K.; Aghzzaf, A.A.; Chraka, A.; Aznag, B.; Chaouket, F.; Bouchta, D. Anticorrosive performance of lanthanum ions intercalated Stevensite clay on brass in 3% NaCl medium. *Mater. Today Proc.* **2020**, *22*, 78–82. [CrossRef]
11. Hu, T.; Shi, H.; Wei, T.; Liu, F.; Fan, S.; Han, E.H. Cerium tartrate as a corrosion inhibitor for AA 2024-T3. *Corros. Sci.* **2015**, *95*, 152–161. [CrossRef]
12. Zarrouk, A.; Hammouti, B.; Lakhlifi, T.; Traisnel, M.; Vezin, H.; Bentiss, F. New 1H-pyrrole-2,5-dione derivatives as efficient organic inhibitors of carbon steel corrosion in hydrochloric acid medium: Electrochemical, XPS and DFT studies. *Corros. Sci.* **2015**, *90*, 572–584. [CrossRef]
13. Boughoues, Y.; Benamira, M.; Messaadia, L.; Ribouh, N. Adsorption and corrosion inhibition performance of some environmental friendly organic inhibitors for mild steel in HCl solution via experimental and theoretical study. *Colloids Surf. A Physicochem. Eng. Asp.* **2020**, *593*, 124610. [CrossRef]
14. Yadav, M.; Kumar, S.; Sinha, R.R.; Bahadur, I.; Ebenso, E.E. New pyrimidine derivatives as efficient organic inhibitors on mild steel corrosion in acidic medium: Electrochemical, SEM, EDX, AFM and DFT studies. *J. Mol. Liq.* **2015**, *211*, 135–145. [CrossRef]
15. Obot, I.B.; Ankah, N.K.; Sorour, A.A.; Gasem, Z.M.; Haruna, K. 8-Hydroxyquinoline as an alternative green and sustainable acidizing oilfield corrosion inhibitor. *Sustain. Mater. Technol.* **2017**, *14*, 1–10. [CrossRef]
16. Selvi, S.T.; Raman, V.; Rajendran, N. Corrosion inhibition of mild steel by benzotriazole derivatives in acidic medium. *J. Appl. Electrochem.* **2003**, *33*, 1175–1182. [CrossRef]
17. Rihan, R.; Shawabkeh, R.; Al-Bakr, N. The Effect of Two Amine-Based Corrosion Inhibitors in Improving the Corrosion Resistance of Carbon Steel in Sea Water. *J. Mater. Eng. Perform.* **2013**, *23*, 693–699. [CrossRef]
18. Quartarone, G.; Bonaldo, L.; Tortato, C. Inhibitive action of indole-5-carboxylic acid towards corrosion of mild steel in deaerated 0.5 M sulfuric acid solutions. *Appl. Surf. Sci.* **2006**, *252*, 8251–8257. [CrossRef]
19. Cen, H.; Cao, J.; Chen, Z.; Guo, X. 2-Mercaptobenzothiazole as a corrosion inhibitor for carbon steel in supercritical CO_2-H_2O condition. *Appl. Surf. Sci.* **2019**, *476*, 422–434. [CrossRef]
20. Snihirova, D.; Lamaka, S.V.; Montemor, M.F. "SMART" protective ability of water based epoxy coatings loaded with $CaCO_3$ microbeads impregnated with corrosion inhibitors applied on AA2024 substrates. *Electrochim. Acta* **2012**, *83*, 439–447. [CrossRef]
21. Dkhireche, N.; Galai, M.; Ouakki, M.; Rbaa, M.; Ech-chihbi, E.; Lakhrissi, B.; EbnTouhami, M. Electrochemical and theoretical study of newly quinoline derivatives as a corrosion inhibitors adsorption onmild steel in phosphoric acid media. *Inorg. Chem. Commun.* **2020**, *121*, 108222. [CrossRef]

22. Snihirova, D.; Lamaka, S.V.; Cardoso, M.M.; Condeço, J.A.D.; Ferreira, H.E.C.S.; Montemor, M.d. pH-sensitive polymeric particles with increased inhibitor-loading capacity as smart additives for corrosion protective coatings for AA2024. *Electrochim. Acta* **2014**, *145*, 123–131. [CrossRef]
23. Li, W.; He, Q.; Pei, C.; Hou, B. Experimental and theoretical investigation of the adsorption behaviour of new triazole derivatives as inhibitors for mild steel corrosion in acid media. *Electrochim. Acta* **2007**, *52*, 6386–6394. [CrossRef]
24. Taryba, M.; Lamaka, S.V.; Snihirova, D.; Ferreira, M.G.S.; Montemor, M.F.; Wijting, W.K.; Toews, S.; Grundmeier, G. The combined use of scanning vibrating electrode technique and micro-potentiometry to assess the self-repair processes in defects on "smart" coatings applied to galvanized steel. *Electrochim. Acta* **2011**, *56*, 4475–4488. [CrossRef]
25. Snihirova, D.; Lamaka, S.V.; Taryba, M.; Salak, A.N.; Kallip, S.; Zheludkevich, M.L.; Ferreira, M.G.S.; Montemor, M.F. Hydroxyapatite microparticles as feedback-active reservoirs of corrosion inhibitors. *ACS Appl. Mater. Interfaces* **2010**, *2*, 3011–3022. [CrossRef] [PubMed]
26. Qian, B.; Michailidis, M.; Bilton, M.; Hobson, T.; Zheng, Z.; Shchukin, D. Tannic complexes coated nanocontainers for controlled release of corrosion inhibitors in self-healing coatings. *Electrochim. Acta* **2019**, *297*, 1035–1041. [CrossRef]
27. Chang, J.; Wang, Z.; Han, E.h.; Liang, X.; Wang, G.; Yi, Z.; Li, N. Corrosion resistance of tannic acid, d-limonene and nano-ZrO_2 modified epoxy coatings in acid corrosion environments. *J. Mater. Sci. Technol.* **2021**, *65*, 137–150. [CrossRef]
28. Raj, R.; Taryba, M.G.; Morozov, Y.; Kahraman, R.; Shakoor, R.A.; Montemor, M.F. On the synergistic corrosion inhibition and polymer healing effects of polyolefin coatings modified with Ce-loaded hydroxyapatite particles applied on steel. *Electrochim. Acta* **2021**, *388*, 138648. [CrossRef]
29. Yuan, Q.; Qin, C.; Wu, J.; Xu, A.; Zhang, Z.; Liao, J.; Lin, S.; Ren, X.; Zhang, P. Synthesis and characterization of Cerium-doped hydroxyapatite/polylactic acid composite coatings on metal substrates. *Mater. Chem. Phys.* **2016**, *182*, 365–371. [CrossRef]
30. Rehman, I.; Bonfield, W. Characterization of hydroxyapatite and carbonated apatite by photo acoustic FTIR spectroscopy. *J. Mater. Sci. Mater. Med.* **1997**, *8*, 1–4. [CrossRef]
31. Kandori, K.; Oketani, M.; Sakita, Y.; Wakamura, M. FTIR studies on photocatalytic activity of Ti(IV)-doped calcium hydroxyapatite particles. *J. Mol. Catal. A Chem.* **2012**, *360*, 54–60. [CrossRef]
32. Xia, Z.; Singh, A.; Kiratitanavit, W.; Mosurkal, R.; Kumar, J.; Nagarajan, R. Unraveling the mechanism of thermal and thermo-oxidative degradation of tannic acid. *Thermochim. Acta* **2015**, *605*, 77–85. [CrossRef]
33. Zhang, N.; Luo, J.; Liu, R.; Liu, X. Tannic acid stabilized silver nanoparticles for inkjet printing of conductive flexible electronics. *RSC Adv.* **2016**, *6*, 83720–83729. [CrossRef]